JOURNAL OF VIROLOGY, Aug. 2007, p. 8050–8062 Vol. 81, No. 15
0022-538X/07/$08.00+0 doi:10.1128/JVI.00249-07

Insulin-Like Growth Factor II Receptor-Mediated Intracellular Retention of Cathepsin B Is Essential for Transformation of Endothelial Cells by Kaposi's Sarcoma-Associated Herpesvirus▽

Patrick P. Rose,[1] Matthew Bogyo,[2] Ashlee V. Moses,[1] and Klaus Früh[1]*

Vaccine and Gene Therapy Institute, Oregon Health and Science University, Portland, Oregon 97239,[1] and Stanford University School of Medicine, Stanford, California 94305-5324[2]

Received 5 February 2007/Accepted 8 May 2007

Kaposi's sarcoma-associated herpesvirus (KSHV) is the pathological agent of Kaposi's sarcoma (KS), a tumor characterized by aberrant proliferation of endothelial-cell-derived spindle cells. Since in many cancers tumorigenesis is associated with an increase in the activity of the cathepsin family, we studied the role of cathepsins in KS using an in vitro model of KSHV-mediated endothelial cell transformation. Small-molecule inhibitors and small interfering RNA (siRNA) targeting CTSB, but not other cathepsins, inhibited KSHV-induced postconfluent proliferation and the formation of spindle cells and foci of dermal microvascular endothelial cells. Interestingly, neither CTSB mRNA nor CTSB protein levels were induced in endothelial cells latently infected with KSHV. Secretion of CTSB was strongly diminished upon KSHV infection. Increased targeting of CTSB to endosomes was caused by the induction by KSHV of the expression of insulin-like growth factor-II receptor (IGF-IIR), a mannose-6-phosphate receptor (M6PR) that binds to cathepsins. Inhibition of IGF-IIR/M6PR expression by siRNA released CTSB for secretion. In contrast to the increased cathepsin secretion observed in most other tumors, viral inhibition of CTSB secretion via induction of an M6PR is crucial for the transformation of endothelial cells.

Kaposi's sarcoma-associated herpesvirus/human herpesvirus 8 (KSHV/HHV8) belongs to the gammaherpesvirus subfamily and is the pathological agent of Kaposi's sarcoma (KS) and of lymphoproliferative disorders in B cells (20). KS is a mesenchymal tumor generally targeting the skin and soft tissue organs. The sarcoma is composed of interweaving bands of vascularizing spindle cells of endothelial origin, frequently associated with infiltrating inflammatory cells (8, 35). AIDS has been most commonly associated with KS, although other forms of KS exist independently of human immunodeficiency virus infection, e.g., classic, endemic, and iatrogenic KS (15, 35). Antiretroviral treatments against human immunodeficiency virus have effectively reduced the prevalence of AIDS-associated KS; however, the incidence of iatrogenic KS has increased 400% relative to the population growth in North America. This is most likely due to an increase in the number of organ transplant recipients (46).

The development of several in vitro systems that rely on infection of primary or immortalized endothelial cells by KSHV has greatly advanced our understanding of virus-host cell interaction during tumorigenesis (31). Dermal microvascular endothelial cells stably transfected with the oncogenes E6 and E7 of human papillomavirus (E-DMVEC) are immortalized but remain contact inhibited, grow as discrete monolayers with a cobblestone phenotype, and enter senescence if not passaged after attaining confluence (37). Upon infection with KSHV, E-DMVEC develop a spindle cell phenotype, lose contact inhibition, form foci when cultured postconfluence, and acquire the ability to form colonies in soft agar (37). As in KS tumors, viral gene expression in E-DMVEC is largely restricted to open reading frame 71 (ORF71 [vFLIP]), ORF72 (vCyclin), ORF73 (latency-associated nuclear antigen [LANA]), and kaposin, and only a few cells spontaneously enter the lytic cycle of viral replication. Despite the restricted viral gene expression program, latent infections are associated with a dramatic reprogramming of the cellular transcriptome and proteome (4, 38, 39, 55). Several virus-induced host cell proteins are required to support postconfluent growth, including c-Kit, hemoxygenase, RDC-1, Neuritin, and the insulin receptor (30, 39, 42, 43).

One of the hallmarks of KS is aberrant neoangiogenesis by proliferating spindle cells, resulting in abnormal vasculature. Neoangiogenesis involves the degradation of extracellular matrix by proteases, a process that frequently involves cysteine proteases of the cathepsin family (6, 21, 22, 53). Despite this important role of cathepsins in many cancers, the role of cathepsin function in KS development has not been studied so far. Cathepsins are part of the papain subfamily within the cysteine protease superfamily. Most cathepsins are ubiquitously expressed in lysosomes and play a role in protein degradation and processing. In addition to these housekeeping functions, cathepsins are implicated in a wide variety of diseases, including cancer (53, 54). In particular, cathepsin B (CTSB) is linked to a number of human cancers, including prostate carcinoma, breast cancer, and brain tumors (19, 27, 49, 51, 57).

In an effort to characterize cathepsin involvement in KSHV-induced tumorigenesis, we now demonstrate that CTSB is an essential factor for KSHV-induced postconfluent growth of E-DMVEC whereas other cathepsins tested did not play an

* Corresponding author. Mailing address: Vaccine and Gene Therapy Institute, Oregon Health and Science University, 505 NW 185th Ave., Beaverton, OR 97006. Phone: (503) 418-2735. Fax: (503) 418 2701. E-mail: fruehk@ohsu.edu.

▽ Published ahead of print on 16 May 2007.

essential role. Unexpectedly, secretion of CTSB was inhibited in latently infected endothelial cells. CTSB is retained by the insulin-like growth factor-II receptor/mannose-6-phosphate receptor (IGF-IIR/M6PR), which we previously reported to be transcriptionally induced during KSHV-mediated transformation of E-DMVEC (43). Therefore, in contrast to the increased secretion of CTSB observed in several other tumor models, CTSB is retained in the endosomal/lysosomal compartment in KS, where it likely regulates the processing of growth factors or growth factor binding proteins. Given the recent progress in developing CTSB inhibitors for cancer treatment (10), our data suggest that such inhibitors might be a novel treatment for KS.

MATERIALS AND METHODS

Viruses, cell culture, and reagents. KSHV-infected E-DMVEC were established and maintained as previously described (37). KSHV-infected DMVEC were used in experiments when >90% of the cells expressed LANA-1. CA-074 (catalog no. 205530), CA-074ME (catalog no. 205531), and hydroxy-2-naphthalenyl-methyl phosphonic acid trisacetoxymethyl ester [HNMPA-(AM_3)] (catalog no. 397100) were obtained from EMD Biosciences (San Diego, CA). Antibodies against cathepsin S (catalog no. IM1003), cathepsin L (catalog no. 219387), and CTSB (catalog no. IM27L) were purchased from EMD Biosciences (San Diego, CA). A mouse monoclonal antibody against calreticulin (SPA-601) was purchased from Stressgen (Victoria, British Columbia, Canada). Purified human native CTSB (catalog no. JA7741) was obtained from EMD Biosciences (San Diego, CA). A polyclonal antibody against IGF-IIR/M6PR (H-20) was obtained from Santa Cruz Biotechnology (Santa Cruz, CA).

Microarray experiments and analysis. cDNA synthesis, hybridization to HG_U133A and B arrays (Affymetrix), and signal intensity normalization were performed at the Oregon Health and Science University (OHSU) microarray core facility (www.ohsu.edu/gmsr/amc). GeneChip data were analyzed with Arrayassist (Stratagene). Comparisons were made between passage-matched KSHV-infected E-DMVEC and mock-infected E-DMVEC in four separate experiments. A master data table consisting of expression values extracted from all CEL files was created by the probe logarithmic error intensity estimate (PLIER) method. To define the baseline from which changes in gene expression data were determined for KSHV-infected samples, a virtual chip comprising all mock-infected control expression data was used. Significant changes with a P value of 0.01 were determined by analysis of variance with variance stabilization and no P value correction.

Western blotting and immunoprecipitations. For immunoprecipitation, cells were washed twice with ice-cold phosphate-buffered saline (PBS) and lysed in NP-40 buffer (1% NP-40, 150 mM NaCl, 10% glycerol, 20 mM Tris-HCl [pH 8.0], 1 mM EDTA [pH 8.0], 0.2% sodium dodecyl sulfate [SDS]) containing protease inhibitors (Roche Diagnostics; Indianapolis, IN), 1 mM $NaVO_4$, and 1 mg/ml pepstatin. Lysates were cleared, and the protein concentration was determined. For IGF-IIR/M6PR, 500 μg of whole-cell lysate protein was immunoprecipitated with 10 μg of an anti-IGF-IIR/M6PR antibody and incubated overnight at 4°C with rocking. A 50-μl volume of a protein A/G-agarose bead slurry (Upstate) was added for 45 min with rocking at 4°C. Three washes were performed, and the pellet was boiled in 2× SDS sample buffer. The beads were spun down, and the supernatant was separated by 10% SDS-polyacrylamide gel electrophoresis. For Western blotting, cells were directly lysed in 1× SDS sample buffer (100 mM Tris-Cl [pH 6.8], 2% SDS, 10% glycerol) without dyes or with dithiothreitol–2-mercaptoethanol and were subsequently boiled for 5 min. Protein content was normalized and determined using a bicinchoninic acid protein assay kit (catalog no. 23227; Pierce, Rockford, IL). Before resolution of samples by 10% SDS-polyacrylamide gel electrophoresis, 100 mM dithiothreitol and 0.01% bromophenol blue were added to the lysates and samples were boiled for 5 min. Gels were transferred to nylon membranes, blocked for 20 min with 10% milk in 1× PBS supplemented with 0.1% Tween 20, and probed with the respective antibodies. Bound antibodies were detected by enhanced chemiluminescence (Pierce) and exposed to film.

Reverse transcriptase PCR (RT-PCR). Quantitative PCR was performed on an ABI7700 sequence detection system (Applied Biosystems, Foster City, CA). Target gene expression was compared to expression of the glyceraldehyde-3-phosphate dehydrogenase housekeeping gene. Total RNA was purified from primary DMVEC using RNeasy spin columns (QIAGEN Inc, Valencia, CA). Human tissue was a generous gift from H. Koon and B. J. Dezube and was prepared as previously described (42). Total RNA was treated with DNase I (DNase free; Ambion, Austin, TX) before synthesis of cDNA with random hexamers and Superscript III (Invitrogen, Carlsbad, CA). The following primers were selected by using Primer Express software (Applied Biosystems): IGF-IIR/M6PR 6333F (GCAGAAGCTGGGTGTCATAGG), 6420R (5′-CACGGAGG ATGCGGTCTTAT), IGF-IR 2184F (GGAGGAGGCTGAATACCGC), and 2252R (5′-TCAGGTCTGGGCACGAAGAT). Reactions were performed using SYBR green PCR core reagents. Relative expression values for uninfected versus KSHV-infected cells and for normal skin versus KS tissue were calculated by the comparative C_T method (28). Dissociation curves were performed on human reference RNA after each amplification run to control for primer dimers. For analysis of CTSB splicing, the following primers were used as previously published for PCR: CTSB full length fwd (5′-CAGCGCTGGGCTGGTGTG), CTSB(−2) fwd (5′-CAGCGCTGGGTGGATCTA), CB(−2/3) fwd (5′-CAGC GCTGGGCCGGGCAC), and CB EXON 11 rev (5′-CCAGGACTGGCACGA CAGGC). PCR to determine CTSB isoforms was performed by standard approaches (95°C for 5 min; 30 cycles of 95°C for 1 min, 55°C for 1 min, and 72°C for 2 min; and 72°C for 10 min).

siRNA treatments. KSHV-infected E-DMVEC were seeded the day prior to small interfering RNA (siRNA) treatment at 30% confluence in 35-mm-diameter polystyrene dishes (Corning). On the day of treatment, for each sample, 3 μl Oligofectamine (Invitrogen) was mixed with 12 μl OptiMEM (GIBCO-Invitrogen) for 5 min at room temperature. A mixture of 200 nM SMARTpool siRNA (Dharmacon) and 180 μl OptiMEM was added to the Oligofectamine mixture and incubated for 20 min at room temperature. For IGF-IIR/M6PR siRNA treatment, single sense strand siRNAs were employed: AGACCAGGCUUGC UCUAUAUU (On-Targetplus set 6), CAACUUUCCUCCAUCACAAUU (On-Targetplus set 7), and CGAUACCUCUCAAGUCAAAUU (On-Targetplus set 8) (catalog no. J-010601-06; Dharmacon). Cells were washed once in OptiMEM, and 800 μl OptiMEM was added to the dish prior to addition of 200 μl siRNA mixture. Cells were incubated for 6 h before receiving a second treatment of siRNA as before. Cells were incubated overnight, and the siRNA mixture was removed and replenished with 2 ml of complete medium. siRNA-treated cells were incubated for 4 to 6 days to determine the peak of downmodulation, at which point protein levels were assayed by Western blotting. For long-term observation of phenotypic changes, siRNA-treated cells were treated again with siRNA 1 week after the first treatment to ensure efficient knockdown. One day after the second treatment series, CTSB activity was measured by a zymogen assay.

Focus inhibition assay. KSHV-infected E-DMVEC were seeded at 30 to 50% confluence on 35-mm-diameter dishes (Corning) and treated either with siRNA or with the CTSB small-molecule inhibitor CA-074 or CA-074ME for a 2-week period. Inhibitors (10 μM) were added during the change of medium (every 2 days), whereas a second round of siRNA treatment was performed 7 days after the first treatment to maintain the knockdown of specified genes. For siRNA rescue, 10 ng/ml of native human CTSB was added every 2 days after initial siRNA treatment and continued for 2 weeks total. Cells were examined for spindle cell formation, loss of contact inhibition (a result of adherent foci in the monolayer), or virus-induced cytopathic effect by microscopy. Cells were washed twice in PBS and fixed in 3.7% paraformaldehyde for 20 min before another wash and addition of a coverslip over 80 μl glycerol.

Immunofluorescence microscopy. Cells were washed twice with 1× PBS and fixed with 3.7% formaldehyde (in PBS) for 20 min at room temperature. Cells were then washed twice with 1× PBS and permeabilized with 0.1% Triton X-100 (in PBS) for 5 min. Subsequently, cells were washed three times with 2% PBA (bovine serum albumin in PBS). To measure KSHV infection after inhibitor treatment, cells were probed with a primary rabbit polyclonal antibody against LANA-1 (ORF73) (a gift from Bala Chandran, Rosalind Franklin University, Chicago, IL) at 1:500 for 2 h at 37°C. Cells were washed three times with 2% PBA and then incubated with a goat anti-rabbit secondary antibody conjugated with Alexa Fluor 594 (Molecular Probes, Eugene, OR) at 1:500 for 45 min at 37°C. Images were analyzed with a Nikon fluorescence microscope. For live staining, KSHV-infected E-DMVEC were seeded at confluence on Lab-Tek II 1.5 borosilicate chambered coverglass slides (catalog no. 155382; Electron Microscopy Sciences, Hatfield, PA). The next day, cells were either left untreated or treated with either CA-074 (10 μM), CA-074ME (10 μM), or HNMPA-(AM_3) (50 μM) overnight before being probed with GB-111 FL (1 μM) for 60 min. Images were acquired by Aurelie Snyder of the OHSU Molecular Microbiology and Immunology Research Core Facility (http://www.ohsu.edu/research/core) with an Applied Precision DeltaVision RT image restoration system. This includes the API chassis with a precision-motorized XYZ stage, an Olympus IX-71 inverted fluorescent microscope with standard filter sets, mercury illumination

with an API light homogenizer, a Nikon CoolSnap camera, and DeltaVision software. Deconvolution using the iterative constrained algorithm of Sedat and Agard and additional image processing were performed on a Linux OS platform with the SoftWoRx program. Further technical specifications are available from Applied Precision.

Cell viability assay. Cell viability by ATP determination was measured according to the manufacturer's protocol (Molecular Probes; catalog no. A-22066). KSHV-infected E-DMVEC were treated with either CA-074 (10 μM), CA-074ME (10 μM), or HNMPA-(AM_3) (100 μM) for 4 days in 35-mm-diameter dishes and were lysed in 1% Triton X-100 for 10 min. A D-luciferin–luciferase mixture (5 μl per sample) was added, and the level of ATP was immediately read in a luminometer.

Annexin V-FITC apoptosis detection assay. Apoptosis in uninfected and KSHV-infected E-DMVEC was analyzed with the R&D Systems annexin V-fluorescein isothiocyanate (FITC) apoptosis detection kit (catalog no. TA4638). Cells were washed once in PBS, plated in serum-free medium, and either treated overnight with staurosporine (1 μM), CA-074 (10 μM), or CA-074ME (10 μM) or left untreated. Cells were trypsinized and washed in 2% PBA before each sample was resuspended in 100 μl annexin reagent (10 μl 10× binding buffer, 10 μl propidium iodide, 1 μl annexin V-FITC, and 79 μl double-distilled H_2O) for 15 min at room temperature. A 400-μl volume of 1× binding buffer was added before samples were analyzed by flow cytometry.

Proliferation assay. Uninfected or KSHV-infected E-DMVEC were seeded at 3×10^5 cells (for preconfluence) or 5×10^5 cells (for postconfluence) per 35-mm-diameter dish. Cells were grown in the presence or absence of CA-074 (10 μM), CA-074ME (10 μM), or HNMPA-(AM_3) (50 μM) for 5 days before being trypsinized, stained with trypan blue, and counted. For the postconfluence assay, cell numbers were normalized to cell numbers in a confluent monolayer of uninfected E-DMVEC (set at 100%) and are presented as percentages of the number of uninfected E-DMVEC.

Soft agar assay. Forty thousand KSHV-infected E-DMVEC, either treated with CA-074 or CA-074ME or left untreated for 14 days, were plated in 1.5 ml endothelial-SFM growth medium (11111-044; Invitrogen) supplemented with 10% human AB serum, 25 μg/ml endothelial cell growth supplement, and 0.4% melted agarose onto a 3-ml bottom layer of 0.5% agarose medium per well of a six-well dish. The cells were fed several drops of medium every 3 days, and colonies were photographed after 3 weeks.

Zymogen assay. CTSB activity was measured with the InnoZyme CTSB activity assay kit (catalog no. CBA001; EMD Biosciences, San Diego, CA). To test inhibition by CA-074 and CA-074ME on native CTSB, 10 μM of either inhibitor was combined with 50 ng of native CTSB enzyme in vitro. The fluorogenic substrate *Z*-Arg-Arg 7-amino-4-methylcoumarin (AMC) was added, and the release of AMC was assayed as recommended by the manufacturer. To measure CTSB enzymatic activity in uninfected and KSHV-infected E-DMVEC lysates and supernatants, cells were seeded in 35-mm-diameter dishes (Corning) in 200 μl medium. Dishes were rocked constantly to cover all cells with medium. The medium was collected, and cells were lysed as suggested in the protocol. Fluorescence was measured using the Flexstation plate reader and analyzed using Softworx Pro (version 4.0.1) software (Molecular Devices, Sunnyvale, CA).

RESULTS

Cathepsins expressed in KSHV-infected E-DMVEC are required for postconfluent growth. Since cathepsins have been implicated in a variety of human cancers, we wanted to assess the role of cathepsins in KSHV-mediated tumorigenesis by using the E-DMVEC in vitro model. We initially monitored postconfluent growth of E-DMVEC latently infected with KSHV in the presence or absence of the broad-spectrum cysteine protease inhibitor (2*S*,3*S*)-*trans*-epoxysuccinyl-L-leucylamido-3-methylbutane ethyl ester loxistatin (EST). KSHV-infected E-DMVEC were seeded at 30% confluence and treated with EST (58 μM) for 2 weeks; the inhibitor was refreshed every third day. While untreated cells develop a spindle cell phenotype and form foci, EST prevented postconfluent growth and caused KSHV-infected E-DMVEC to remain cobblestone-like as a single monolayer (Fig. 1A). Similar observations were made with a series of other broad-spectrum cysteine protease inhibitors (data not shown). These studies suggested

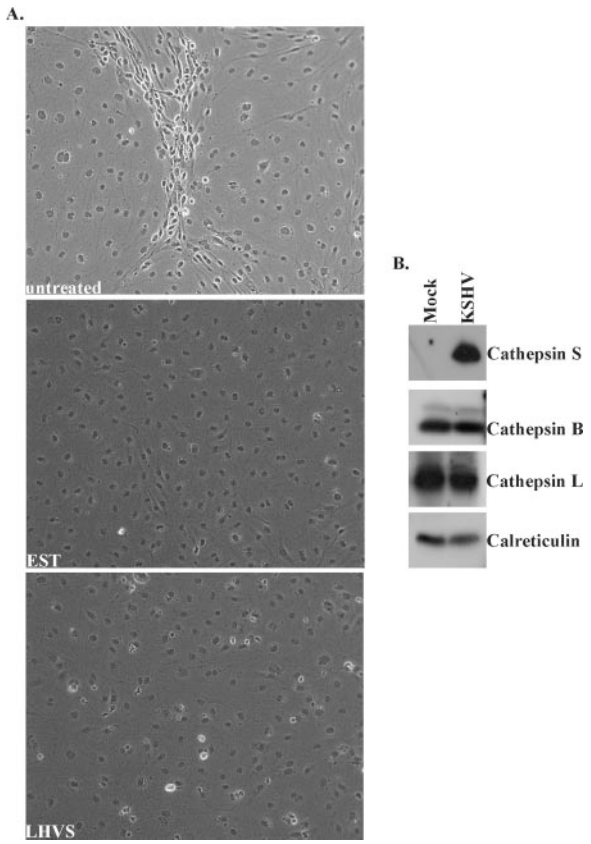

FIG. 1. Cysteine protease inhibitors effectively prevent KSHV-induced formation of spindle cell-containing foci. (A) Phase-contrast images of KSHV-infected E-DMVEC treated with cysteine protease inhibitor EST or LHVS. Both compounds effectively inhibit spindle cell and focus formation. (B) Western blot analysis comparing levels of protein expression for cathepsins S, L, and B in KSHV-infected and uninfected E-DMVEC. To control for equal loading, antibodies to the cellular chaperone calreticulin were used.

that cysteine proteases, presumably cathepsins, are important for the continuous growth of KSHV-infected E-DMVEC when the cells reach confluence.

To determine which cathepsins are expressed in KSHV-infected DMVEC, the gene expression profiles for all known cathepsin transcripts were extracted from complete genome expression arrays (Affymetrix U133A and U133B). Results from four independent experiments with KSHV-infected E-DMVEC cultures were compared with results for their passage- and age-matched cultures of uninfected E-DMVEC. Cathepsin transcripts were scored with the Stratagene algorithm and the PLIER method. Whereas a number of cathepsins were expressed in both uninfected and KSHV-infected E-DMVEC, only cathepsin S, represented by two Affymetrix probe sets, was induced upon KSHV infection (Fig. 2). This expression profile was confirmed at the protein level by using specific antibodies in immunoblotting (Fig. 1B).

siRNA screen against cathepsin S, L, and B suggests CTSB involvement in KSHV-mediated transformation of DMVEC. Using a series of more selective cathepsin inhibitors, we narrowed down the list of potential candidates responsible for the inhibitory effects observed with broad-spectrum inhibitors. In

Gene	Probe Set ID	Infection A	Infection B	Infection C	Infection D
cathepsin B	200838_at	NC	NC	NC	NC
cathepsin B	200839_s_at	NC	NC	NC	NC
cathepsin B	213274_s_at	NC	NC	NC	NC
cathepsin B	213275_x_at	NC	NC	NC	NC
cathepsin C	201487_at	NC	NC	NC	NC
cathepsin F	203657_s_at	NC	NC	NC	NC
cathepsin H	202295_s_at	NC	NC	NC	NC
cathepsin K	202450_s_at	NC	NC	NC	NC
cathepsin L	202087_s_at	NC	NC	NC	NC
cathepsin O	203758_at	NC	NC	NC	NC
cathepsin S*	202901_x_at	I	I	I	I
cathepsin S*	202902_s_at	I	I	I	I
cathepsin V	210074_at	NC	NC	NC	NC
cathepsin W	214450_at	A	A	A	A
cathepsin Z	210042_s_at	A	A	A	A
cathepsin Z	212562_s_at	A	A	A	A
cathepsin D	200766_at	NC	NC	NC	NC
cathepsin G	205653_at	A	A	A	A
cathepsin E	205927_s_at	NC	NC	NC	NC

FIG. 2. Gene expression profiling of cathepsin genes in KSHV-infected and uninfected E-DMVEC. (A) Affymetrix HG_U133A GeneChip data for cathepsins were obtained from four infected samples and compared to their respective controls. Asterisks indicate significant changes ($P > 0.01$ by analysis of variance). Genes with multiple probe sets are reflected in the table. NC, no change in gene expression; A, the probe set scored absent on the microarray; I, changes where gene expression was induced.

particular, the vinyl sulfone LHVS (*N*-morpholinurea-leucine-homophenylalanine-vinylsulfone-phenyl) has specificity for cathepsins S, L, and B (9, 41, 50). KSHV-infected E-DMVEC were treated with LHVS (25 μM) as described above. As with broad-spectrum inhibitors, inhibition of postconfluent growth was observed (Fig. 1A), suggesting that at least one of these proteases is important for KSHV-mediated transformation of E-DMVEC.

To distinguish which of these three cathepsins is necessary for KSHV-induced tumorigenesis, SMARTpool siRNAs were employed against each candidate protease. KSHV-infected E-DMVEC either were treated separately with SMARTpool siRNAs against cathepsin S, L, or B or were mock treated with a Cy3-labeled siRNA against luciferase. siRNA-treated KSHV-infected cultures were monitored over 2 weeks for spindle cell and focus formation. Transfection efficiency was visualized with the Cy3 label conjugated to the luciferase siRNA and was estimated to be consistently around 95%. Western blot analysis of siRNA-treated cultures revealed that all three SMARTpool siRNAs efficiently reduced target protein levels (Fig. 3A). Furthermore, cathepsin L siRNA inhibited its target cathepsin but did not affect protein expression of CTSB, and vice versa. Despite efficient gene knockdown, cathepsin S and L SMARTpool siRNAs did not impede KSHV-induced tumorigenesis. Compared to that for untreated cells, there was a slight reduction in the level of focus formation in cathepsin L and cathepsin S siRNA-treated cells, probably due to the multiple rounds of transfection, since a reduction was also observed with Cy3-labeled control siRNA (not shown). In contrast, CTSB siRNA dramatically inhibited spindle cell and focus development in KSHV-infected E-DMVEC (Fig. 3B). These data suggested that CTSB was responsible for the inhibition of KSHV-mediated E-DMVEC transformation by cathepsin inhibitors.

Intracellularly active CTSB is essential for transformation of DMVEC by KSHV. We initially hypothesized that secreted or extracellular matrix-associated CTSB was involved in tumorigenesis by degrading extracellular matrix components (25, 33, 49). To test this hypothesis, we examined whether postconfluent growth of CTSB siRNA-treated cells could be rescued by exogenous addition of native human CTSB to the medium

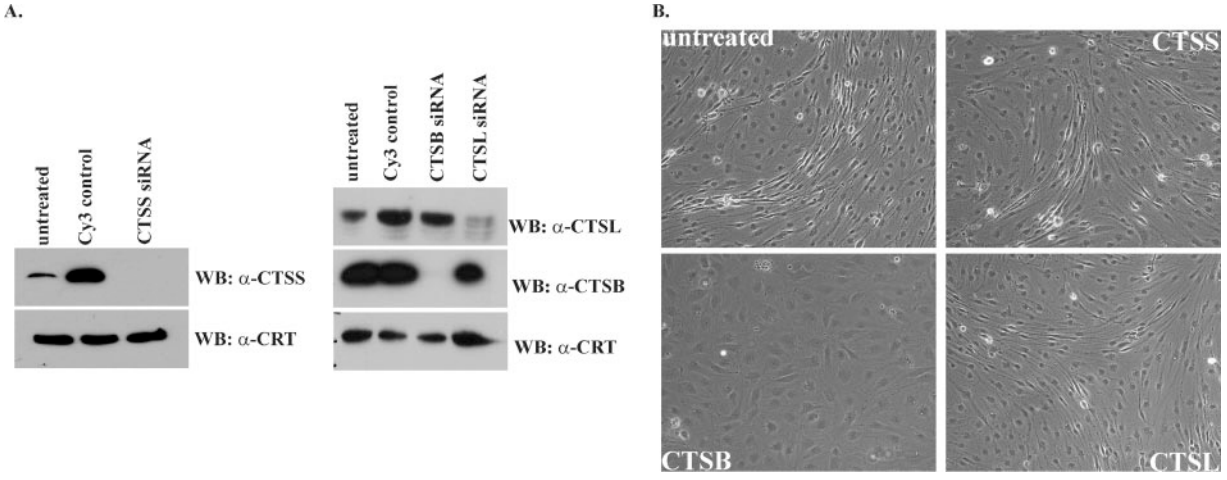

FIG. 3. Downregulation of CTSB mRNA inhibits KSHV-mediated focus formation. (A) Western blot (WB) analysis of cathepsin S, L, and B protein levels after siRNA treatment. An antibody to calreticulin (α-CRT) was used to control for equal loading. siRNAs to cathepsins L and B were target specific as determined by Western blotting. (B) Representative phase-contrast microscopy comparing untreated samples to cathepsin S, L, or B siRNA-treated, KSHV-infected E-DMVEC. Control siRNA-treated samples were indistinguishable from untreated samples and are not represented here. Only CTSB siRNA reduced focus formation. Immunofluorescence analysis of Cy3-labeled siRNA transfectants indicated a transfection efficiency of >95% (data not shown).

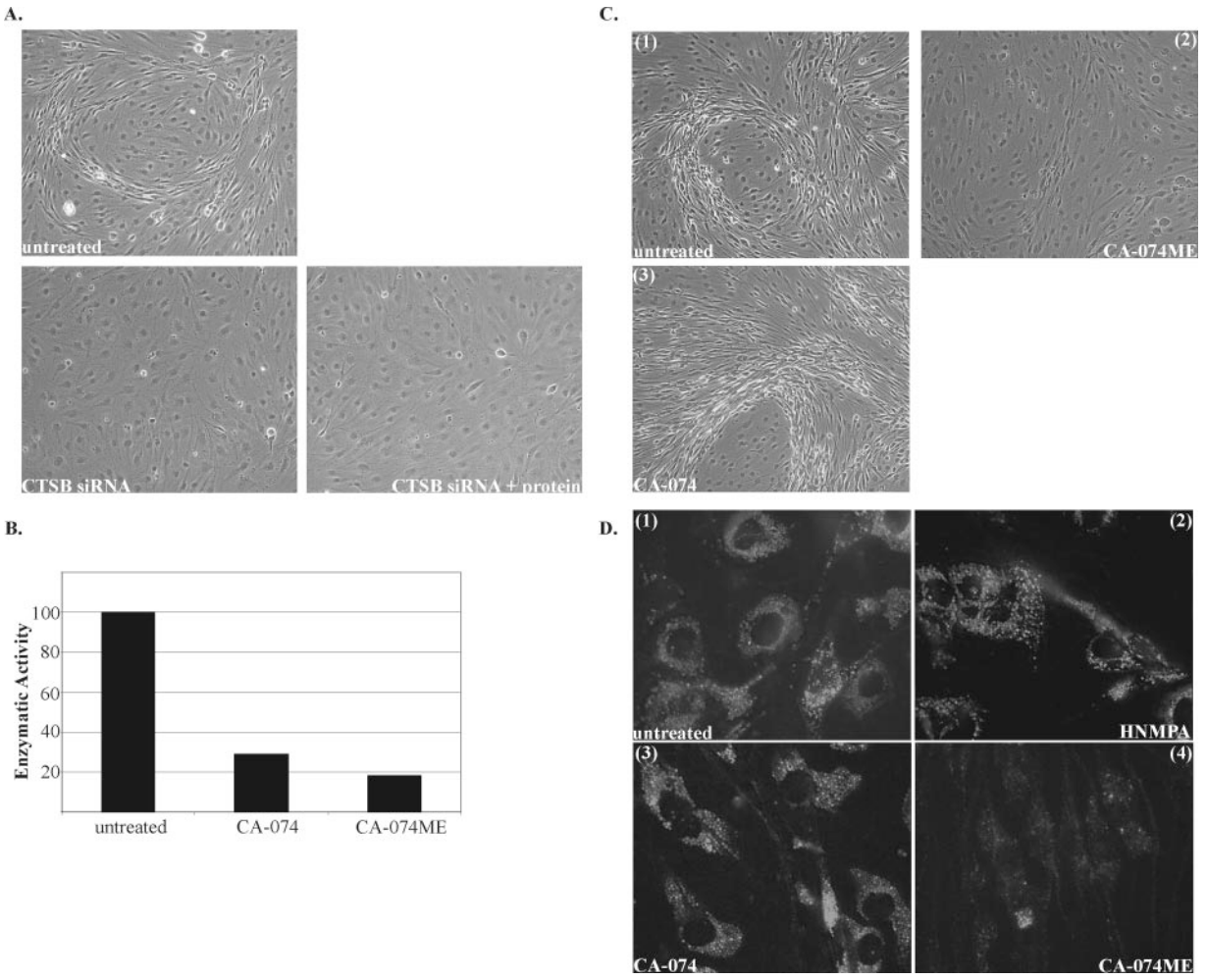

FIG. 4. Intracellular CTSB is essential for KSHV-induced spindle cell and focus formation. (A) Phase-contrast images of CTSB siRNA-treated cultures incubated with purified human native CTSB. Treatment of KSHV-infected E-DMVEC with 10 ng/ml native CTSB (rescue) did not reverse the effect of CTSB siRNA knockdown. The upper left panel shows KSHV-infected E-DMVEC without treatment. (B) Zymogen assay to determine the effectiveness of the two inhibitors of CTSB enzymatic activity. Analysis by cleavage of the CTSB fluorogenic substrate AMC showed that both inhibitors effectively reduced CTSB activity. (C) Representative phase-contrast images of KSHV-infected E-DMVEC that were either left untreated (panel 1) or treated with CA-074ME (panel 3) or CA-074 (panel 2). Only the membrane-permeant version of the CTSB inhibitor, CA-074ME, was able to inhibit spindle cell and focus formation in KSHV-infected E-DMVEC (panel 2). (D) Microscopy images of the fluorescently tagged cathepsin L and B activity probe GB-111 FL after treatment with a competitive CTSB inhibitor or a noncompetitive insulin receptor inhibitor [HNMPA-(AM_3)]. KSHV-infected E-DMVEC were treated with the various inhibitors overnight before being probed with the activity-based small-molecule inhibitor GB-111 FL. Only CA-074ME treatment dramatically reduced the staining pattern of GB-111 FL (panel 4). Untreated (panel 1), HNMPA-(AM_3)-treated (panel 2), and CA-074-treated (panel 3) cells showed no change in their staining. Some cells treated with CA-074 did show a reduction in vesicular staining similar to that with CA-074ME, and it has been documented that CA-074 can permeate the cells; however, at this concentration the inhibitor had no effect on KSHV-induced transformation of E-DMVEC.

of KSHV-infected E-DMVEC. Even after prolonged treatment with 10 ng/ml native human CTSB, the siRNA treatment still inhibited postconfluent growth of spindle cells (Fig. 4A), suggesting that endogenous rather than secreted CTSB is essential for KSHV-mediated transformation.

The role of intracellular versus extracellular CTSB was further examined by using two different versions of the activity-based CTSB suicide inhibitor CA-074. CA-074 is unable to cross the cell membrane and consequently can inhibit only extracellular CTSB activity. A methyl ester-modified version of CA-074, proinhibitor CA-074ME, can cross the membrane and inhibit intracellular CTSB, although the modification reduces selectivity for CTSB (34). To ensure that both versions of CA-074 inhibited CTSB activity, they were tested against native human CTSB in vitro. At a concentration of 10 μM, the inhibitors were combined with native human CTSB in the presence of the synthetic fluorogenic CTSB substrate AMC. The release of AMC was measured by fluorescence. Both versions of CA-074 successfully reduced CTSB activity compared to that with no treatment (Fig. 4B). To examine whether CA-074 or CA-074ME inhibited KSHV-mediated transformation of E-DMVEC, uninfected or KSHV-infected E-DMVEC cultures were treated with 10 μM of the respective CTSB inhibitors over a period of 2 weeks. Untreated KSHV-infected E-DMVEC developed a spindle cell morphology and formed foci (Fig. 4C1). The impermeant version of the inhibitor, CA-074,

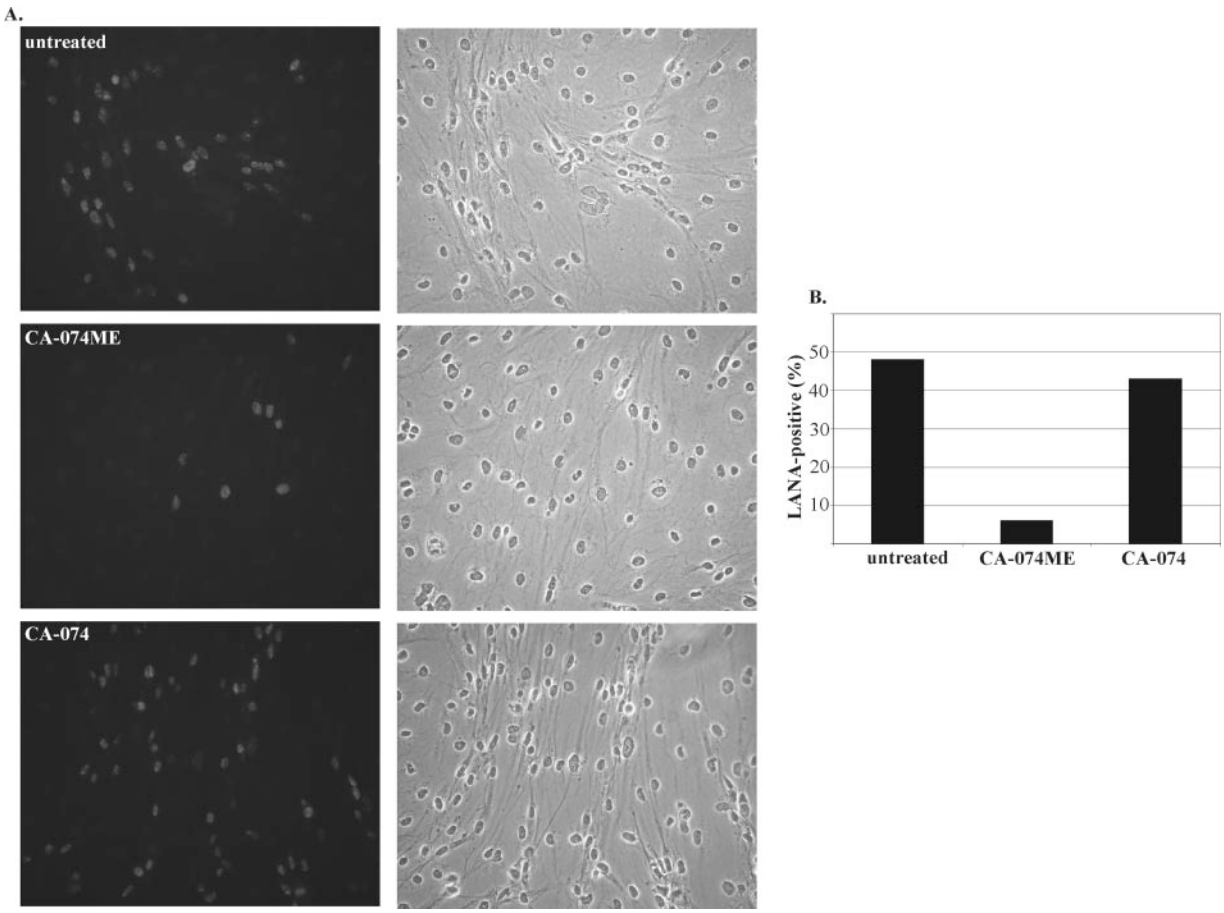

FIG. 5. The membrane-permeant CTSB inhibitor CA-074ME reduces the number of LANA-1-positive E-DMVEC. (A) Phase-contrast and dark-field images of untreated (top), CA-074ME-treated (10 μM) (center), and CA-074-treated (10 μM) (bottom) KSHV-infected E-DMVEC showing expression of LANA-1 in KSHV-infected spindle cells and the selective loss of 89% of LANA-1-positive foci following CA-074ME treatment. (B) Graph quantifying LANA-1-positive cells for each field visualized.

was unable to inhibit spindle cell and focus formation (Fig. 4C3). In contrast, the development of spindle cell morphology was inhibited by CA-074ME (Fig. 4C2). This result supports the conclusion that intracellular rather than secreted CTSB is required for DMVEC transformation by KSHV.

To locate enzymatically active CTSB in live cells, a fluorescein-conjugated activity-based probe, GB-111 FL, which binds to both active cathepsins L and B, was employed. Prior to probing with GB-111 FL, KSHV-infected E-DMVEC were treated with CA-074 (10 μM) or CA-074ME (10 μM). As a control, a noncompetitive inhibitor of the insulin receptor, HNMPA-(AM_3), was used. As shown in Fig. 4D1, untreated cells were probed with GB-111 FL, indicating that active cathepsins L and B are localized to small vesicles. In Fig. 4D2, E-DMVEC treated with the noncompetitive inhibitor HNMPA-(AM_3) showed no difference in staining pattern from untreated cells. Probe staining of most cells treated with the impermeant inhibitor CA-074 was similar to that for untreated cells. Some cells did display reduced vesicular staining (Fig. 4D3). This could be due to the ability of unmodified CA-074 to enter the endocytic compartment during long-term treatment, as has been previously documented (49). The amount that is internalized does not seem to be effective at inhibiting postconfluent growth. In contrast, the membrane-permeant inhibitor CA-074ME completely eliminated vesicular staining (Fig. 4D4), a finding consistent with its efficient inhibition of postconfluent growth. We conclude from these findings that CTSB inhibitors can efficiently neutralize CTSB activity and that intracellular active CTSB is essential for in vitro transformation of DMVEC by KSHV.

The CTSB inhibitor CA-074ME reduces the number of LANA-positive E-DMVEC. In our cell culture system, most but not all E-DMVEC are latently infected with KSHV. However, spindle cell-containing foci forming upon postconfluent growth are enriched for latently infected cells (43). Therefore, we wanted to explore whether treatment with a CTSB inhibitor changed the ratio of infected to uninfected E-DMVEC. Cells were stained for LANA-1, which tethers the viral genome to the cellular chromosome, thus giving a characteristic punctate staining pattern. KSHV-infected E-DMVEC were either left untreated or treated for 14 days with either CA-074 (10 μM) or CA-074ME (10 μM) and then stained with a polyclonal antibody against LANA-1 (Fig. 5A). CA-074ME treatment resulted in a dramatic, 89% reduction in the number of LANA-1 positive cells relative to that of untreated KSHV-infected E-DMVEC (Fig. 5A, center and top), whereas the imperment

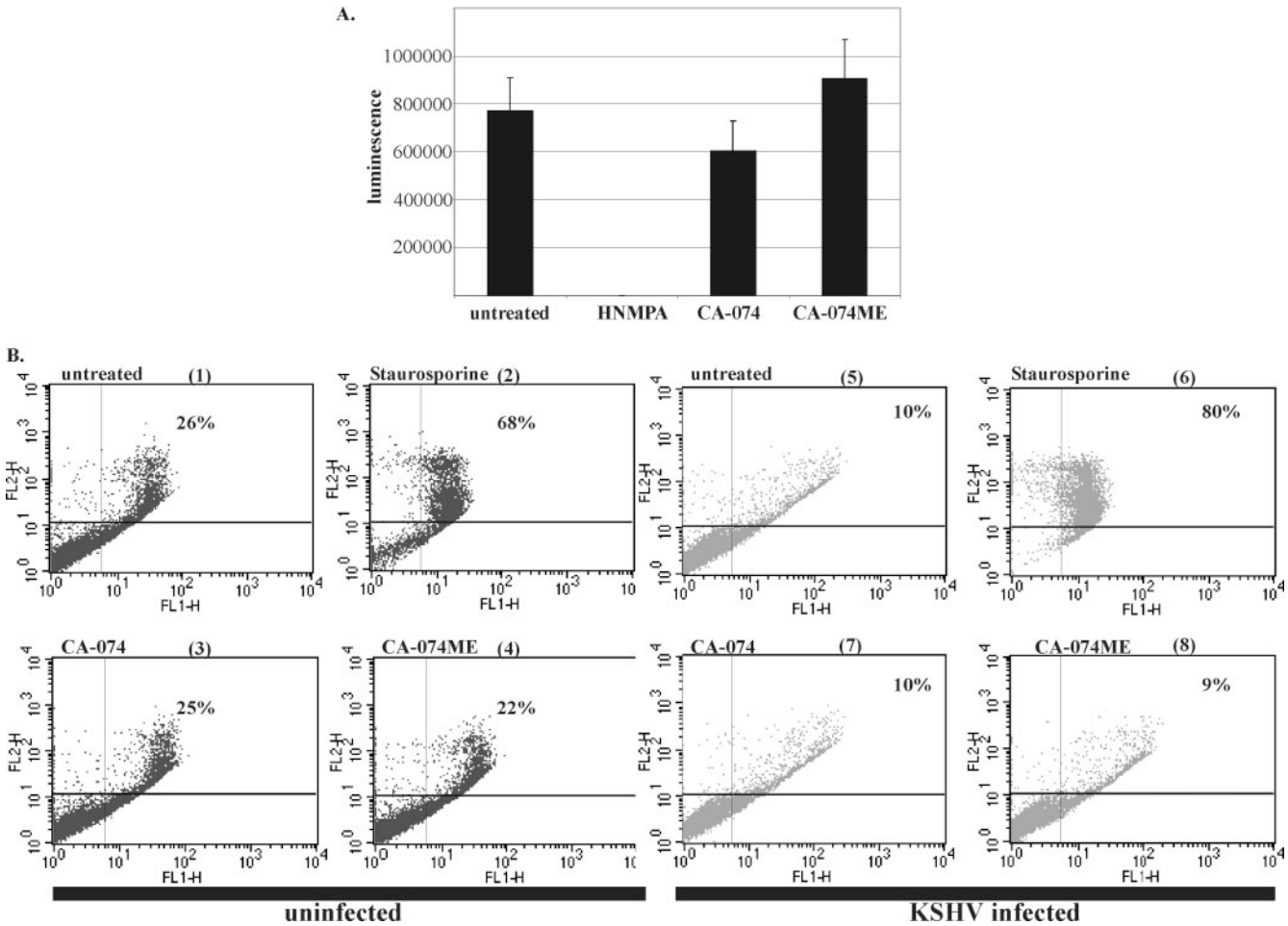

FIG. 6. CTSB inhibitors are nontoxic and do not induce apoptosis. (A) ATP cell viability assay. KSHV-infected E-DMVEC were either left untreated or treated with either 10 μM CA-074, 10 μM CA-074ME, or 100 μM HNMPA-(AM_3). After treatment, cells were lysed, and ATP was quantitatively determined using a luciferin bioluminescence assay. Neither CA-074 nor CA-074ME was toxic to the cells. (B) Annexin V-FITC apoptosis detection assay. Uninfected (panels 1 to 4) and KSHV-infected (panels 5 to 8) E-DMVEC were double-stained with propidium iodide and Annexin V-FITC. No significant difference in apoptosis was seen between untreated cells (panels 1 and 5) and cells treated with 10 μM CA-074 (panels 3 and 7) or CA-074ME (panels 4 and 8). Staurosporine was used as a positive control (panels 2 and 6). Lower left quadrant, healthy cells, lower right, early-apoptotic cells; upper right, late-apoptotic cells.

inhibitor CA-074 did not change the ratio of LANA-1-positive to LANA-1-negative cells (Fig. 5, bottom). The number of LANA-1-positive cells was quantified by counting individual nuclei as shown in Fig. 5B. These observations indicated that the postconfluent growth advantage of LANA-1 positive KSHV-infected E-DMVEC is reduced when CTSB activity is inhibited with CA-074ME.

CTSB inhibitors are nontoxic and do not sensitize KSHV-infected E-DMVEC to apoptosis. To address whether CTSB inhibitors are toxic to cells, an ATP cell viability assay was performed. KSHV-infected E-DMVEC either were cultured in the presence of CA-074 (10 μM) or CA-074ME (10 μM) or were left untreated for 2 weeks. As a positive control, a previously identified inhibitor of KSHV-induced tumorigenesis, HNMPA-(AM_3), was used at a concentration (100 μM) that is toxic to the cells (43). Cells reached confluence and formed spindle cell-containing foci, except when treated with CA-074ME. Treated cells were lysed, and ATP was quantitatively determined by a luciferin bioluminescence assay. A decrease in the ATP concentration was seen only with HNMPA-(AM_3), as previously reported (43). In contrast, neither CA-074 nor CA-074ME seemed to inhibit cell viability (Fig. 6A).

Additionally, CTSB inhibitor-treated cells were assayed by flow cytometry for phospholipid flipping as an indication of apoptosis by using an annexin V-FITC apoptosis detection kit. Cells and supernatants were collected after 14 days of treatment with CA-074 (10 μM) or CA-074ME (10 μM) and were stained with annexin V-FITC and propidium iodide. The staining pattern distinguishes between early-apoptotic cells (positive for annexin V) and late-apoptotic cells (positive for propidium iodide and annexin V). While neither treated (uninfected [Fig. 6B3 and B4] and KSHV infected [Fig. 6B7 and B8]) nor untreated (Fig. 6B1 and B5) E-DMVEC showed any significant change in the number of viable cells, a large double-positive cell population was visible upon treatment with the apoptosis-inducing compound staurosporine (Fig. 6B2 and B6). The ATP viability assay and the annexin V stain show that the CTSB inhibitor concentrations used are not toxic to cells.

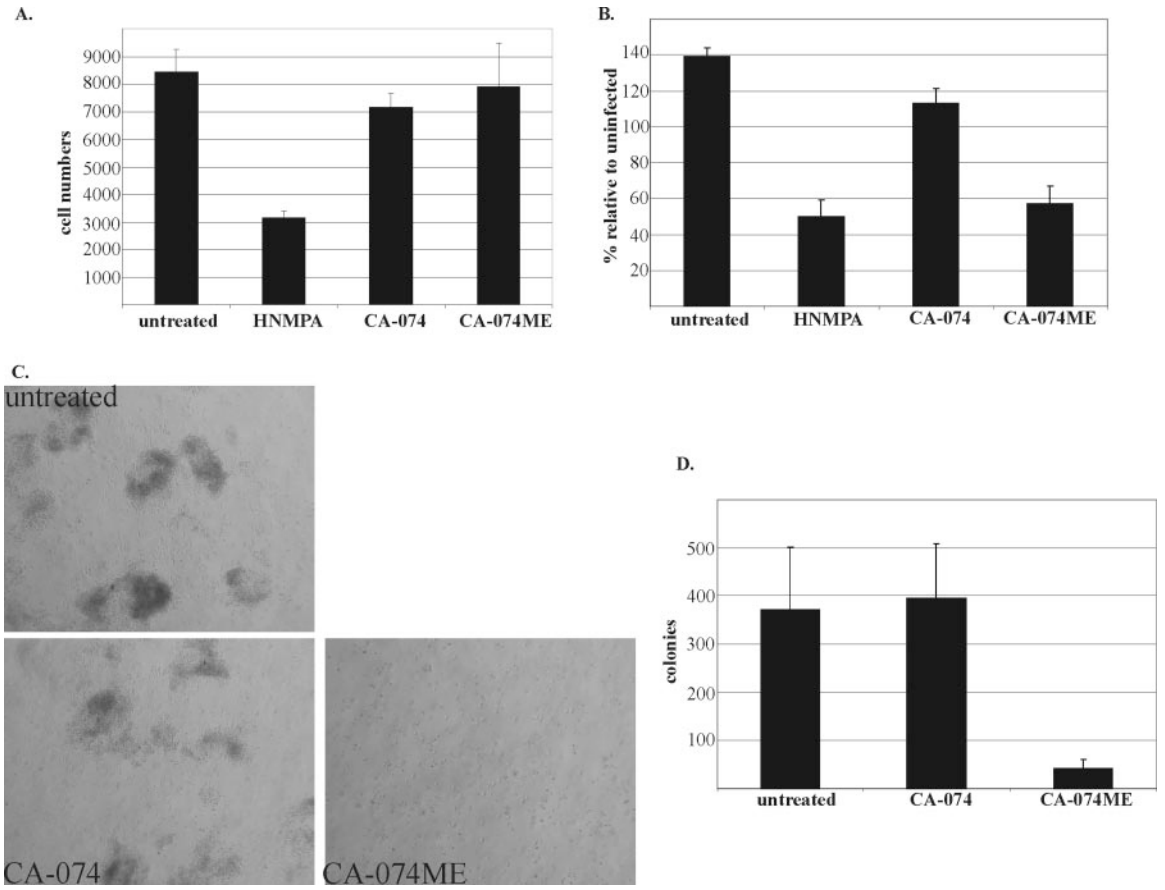

FIG. 7. Inhibiting intracellular CTSB activity prevents postconfluent anchorage-independent growth of KSHV-infected E-DMVEC. (A) Preconfluent cell proliferation. Cells were seeded at a low density and were either left untreated or treated with either CA-074, CA-074ME, or HNMPA-(AM_3). Total-cell counts were determined using a hemocytometer and were compared to normal cell proliferation of untreated E-DMVEC. (B) Postconfluent cell proliferation. Uninfected or KSHV-infected E-DMVEC were seeded at a high density and treated with either CA-074, CA-074ME, or HNMPA-(AM_3). Total-cell numbers of KSHV-infected E-DMVEC, counted using a hemocytometer, are presented as a percentage of uninfected E-DMVEC total-cell counts in order to determine differences based on any effect of CA-074, CA-074ME, or HNMPA-(AM_3) treatment. (C) Soft-agar growth assay. KSHV-infected E-DMVEC were either left untreated or treated with either CA-074 or CA-074ME for 14 days and transferred to a soft-agar-containing medium. Phase-contrast images are representative. (D) Graph quantifies the number of foci observed in each sample; data are means from two replicate experiments.

CTSB supports postconfluent focus formation and loss of contact inhibition. Next, we examined whether CTSB inhibitors affected the proliferation of KSHV-infected E-DMVEC prior to confluence. Cells were seeded at a low density and allowed to grow to confluence while treated with either CA-074 (10 μM), CA-074ME (10 μM), or HNMPA-(AM_3) (100 μM). Cells were trypsinized, stained with trypan blue, and counted using a hemocytometer. Treatment with either version of the CTSB inhibitor CA-074 did not reduce cell numbers (Fig. 7A). As expected, HNMPA-(AM_3) reduced cell numbers. These results support the notion that proliferation of KSHV-infected E-DMVEC is not affected by CTSB inhibitors.

To determine whether the postconfluent growth of KSHV-infected E-DMVEC was affected, cells were seeded at confluence and treated with either CA-074 (10 μM), CA-074ME (10 μM), or HNMPA-(AM_3) (50 μM) for 2 weeks. Cells were trypsinized, stained with trypan blue, and counted using a hemocytometer. Inhibition of intracellular CTSB activity with the methyl ester version of CA-074 dramatically reduced the number of cells in culture. This result is similar to that for the positive-control HNMPA-(AM_3) treatment (at 50 μM). It was shown previously that at this nontoxic concentration, HNMPA-(AM_3) efficiently inhibited KSHV-induced tumorigenesis (43). It appears that CA-074ME similarly targeted KSHV-infected cells to inhibit tumorigenesis. In contrast, KSHV-mediated postconfluent proliferation was not affected by the unmodified version of CA-074 but was comparable to that for untreated KSHV-infected E-DMVEC (Fig. 7B).

KSHV-infected E-DMVEC have the ability to form colonies in soft agar, a hallmark of transformation (37, 43). To establish whether KSHV-infected E-DMVEC were able to form colonies upon CTSB inhibition, cells either were treated with CA-074 (10 μM) or CA-074ME (10 μM) or were left untreated for 14 days before being transferred to soft agar. Both cells treated with CA-074 and untreated KSHV-infected E-DMVEC efficiently formed colonies in soft agar. In contrast, the membrane-permeant CTSB inhibitor CA-074ME inhibited colony formation (Fig. 7C). The total number of colonies formed under each condition is quantified in Fig. 7D. Taken together, the results suggest that CTSB is not required for E-DMVEC

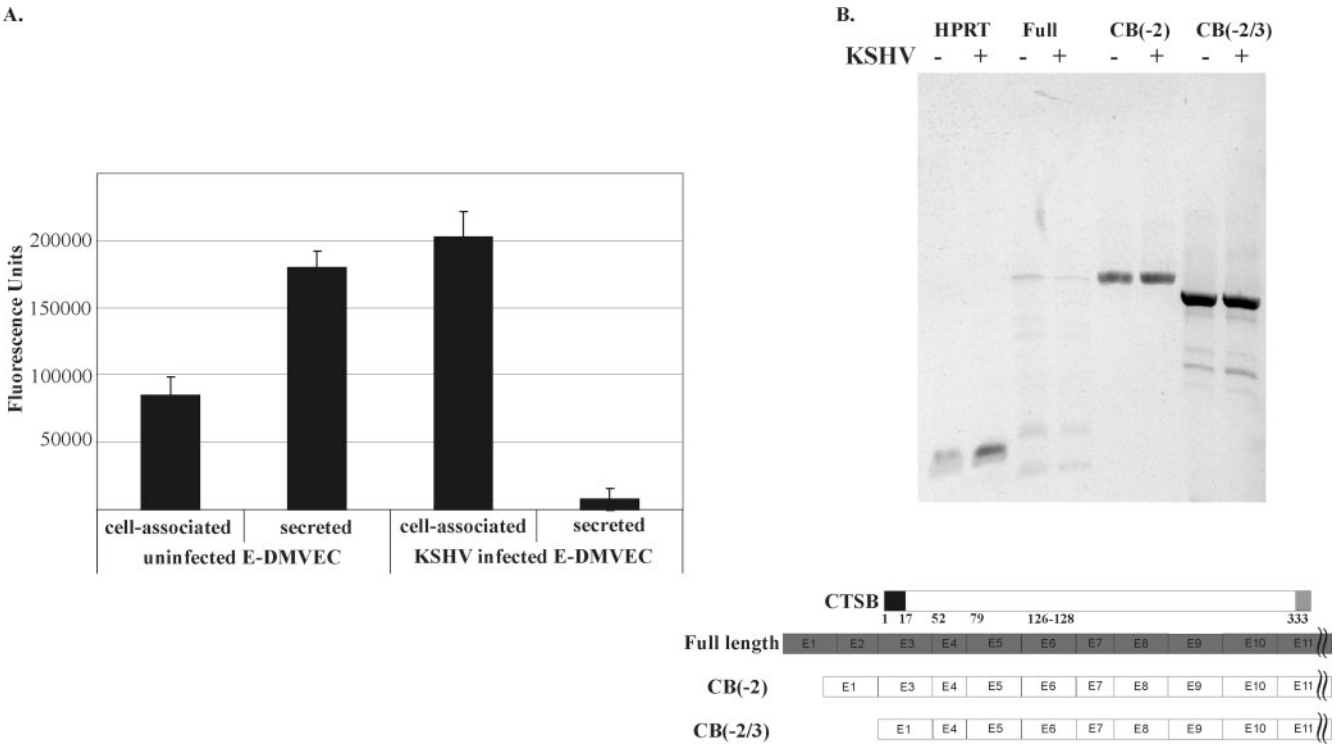

FIG. 8. Active CTSB is retained in KSHV-infected E-DMVEC, and both uninfected and KSHV-infected E-DMVEC express the same CTSB mRNA species. (A) Zymogen assay comparing CTSB enzymatic activities of uninfected and KSHV-infected E-DMVEC cultures in lysates and supernatants. Uninfected E-DMVEC secrete the majority of active CTSB, while KSHV-infected E-DMVEC retain almost all of the active CTSB intracellularly, as very little is secreted. (B) RT-PCR determining CTSB mRNA species in uninfected and KSHV-infected E-DMVEC. The hypoxanthine phosphoribosyltransferase (HPRT) housekeeping gene was used as a positive control. Both uninfected and KSHV-infected cells have truncated versions of CTSB mRNA as the dominant species; they are missing either exon 2 or exons 2 and 3.

proliferation prior to confluence. Instead, CTSB is essential for supporting postconfluent and anchorage-independent growth.

CTSB activity is retained intracellularly in KSHV-infected E-DMVEC. Our data suggest that KSHV infection in E-DMVEC does not alter CTSB gene expression or protein levels, but intracellular CTSB is essential for postconfluent growth. To determine whether intracellularly retained CTSB was enzymatically active, we compared extracellular and intracellular CTSB activity between uninfected and KSHV-infected E-DMVEC using a CTSB zymogen assay. Cells were cultured overnight in a minimal amount of medium, after which both the supernatants and whole-cell lysates were collected. Lysates and supernatants were mixed with the synthetic fluorogenic CTSB substrate AMC, and released AMC was measured by fluorescence. While most of the active CTSB in uninfected E-DMVEC was secreted, almost all of the active CTSB in KSHV-infected E-DMVEC was retained intracellularly (Fig. 8A).

One possible reason for the differential distribution of CTSB was alternative splicing of the CTSB transcript, which contains 13 exons (1, 2, 32, 57). Tumors can contain different species of CTSB mRNA, which can have a dramatic effect on translational efficiency (1) or on cellular trafficking of the translated protein (32). To examine CTSB mRNA splicing, total RNA from uninfected and KSHV-infected E-DMVEC was isolated and analyzed by RT-PCR. Primers were designed against the most dominant CTSB mRNA products as identified in other tumor models: full-length CTSB, CTSB without exon 2 [CB(−2)], or CTSB without exons 2 and 3 [CB(−2/3)] (32). The dominant species in E-DMVEC appeared to be CTSB mRNAs missing exon 2 or both exons 2 and 3, while the full-length transcript was absent. The same splicing pattern was observed in both KSHV-infected and uninfected E-DMVEC (Fig. 8B), suggesting that differential splicing is most likely not responsible for the subcellular distribution of CTSB.

The KSHV-induced M6PR, IGF-IIR/M6PR, is required for retaining CTSB. Fluorescent probes revealed a perinuclear vesicular staining pattern for active CTSB consistent with an endosomal/lysosomal localization (Fig. 4D). To further determine whether CTSB located to these compartments, we disrupted endocytosis by neutralizing the lysosomal pH with NH_4Cl. Treatment with NH_4Cl did not inhibit the enzymatic activity of CTSB in vitro (Fig. 9A). Instead, the absolute intracellular CTSB activity was reduced in both uninfected and KSHV-infected E-DMVEC to the same extent (Fig. 9B), consistent with a lysosomal/endosomal targeting of CTSB.

Lysosomal targeting of CTSB occurs via M6PRs. The major receptor for sorting CTSB to lysosomes is the IGF-IIR/M6PR (14, 44). Interestingly, we previously observed that IGF-IIR/M6PR expression was highly induced in E-DMVEC latently infected by KSHV (43). Moreover, IGF-IIR/M6PR is highly expressed in KS tissue (Fig. 9C). To determine whether CTSB associated with IGF-IIR/M6PR, we immunoprecipitated IGF-IIR/M6PR and probed for CTSB using specific antibodies. CTSB was clearly present in IGF-IIR/M6PR immunoprecipi-

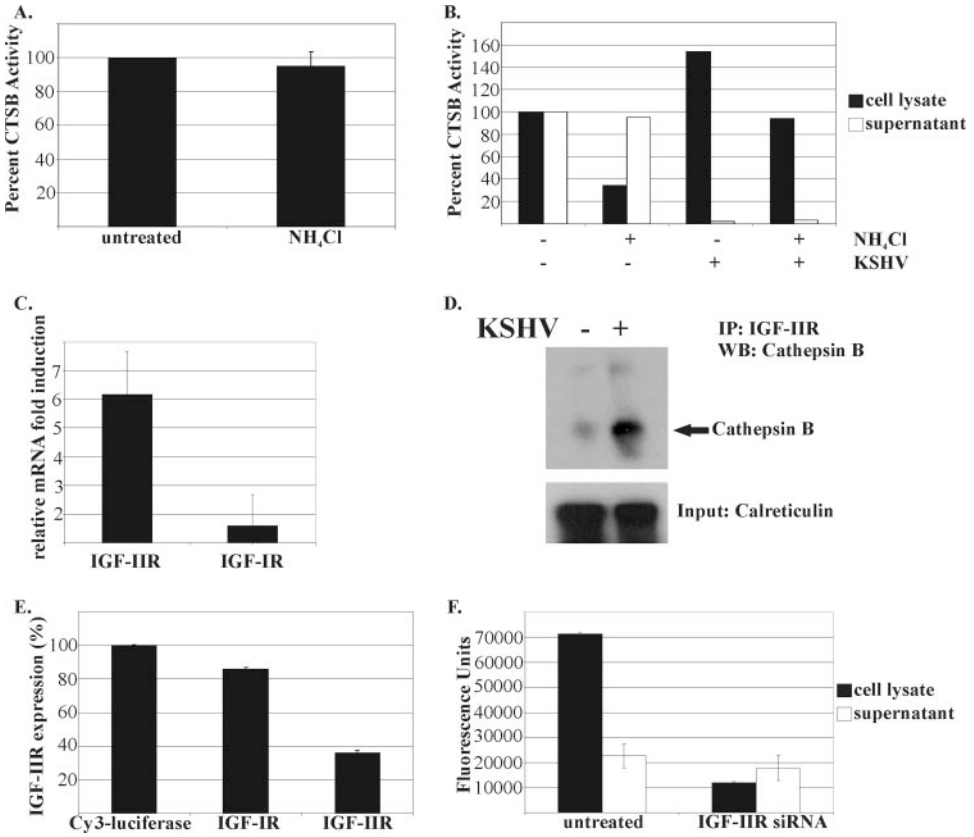

FIG. 9. IGF-IIR/M6PR is responsible for increased endolysosomal trafficking of CTSB. (A) CTSB activity assay after disruption of lysosomes with NH_4Cl. Uninfected and KSHV-infected E-DMVEC lysates and supernatants were collected 24 h after NH_4Cl treatment, and CTSB activity was compared to that for untreated samples. NH_4Cl efficiently disrupted intracellular CTSB activity. (B) CTSB zymogen assay controlling for activity in the presence of NH_4Cl. NH_4Cl had no effect on actual CTSB activity. (C) Quantitative real-time PCR comparing IGF-IR and IGF-IIR/M6PR expression levels in KS tissue. Only IGF-IIR/M6PR was significantly induced in KS tissue. (D) Coimmunoprecipitation of IGF-IIR/M6PR and CTSB. Lysates of uninfected and KSHV-infected E-DMVEC were lysed and immunoprecipitated (IP) with anti-IGF-IIR/M6PR. Samples were resolved on a 10% acrylamide gel and blotted with an anti-CTSB antibody. There was an increase in the level of coimmunoprecipitated CTSB proportional to the increase in IGF-IIR/M6PR expression after long-term KSHV infection. WB, Western blotting. (E) Quantitative real-time PCR confirming efficient knockdown of IGF-IIR/M6PR mRNA after siRNA treatment against IGF-IIR/M6PR. The siRNA had no effect on IGF-IR. (F) Representative assay of CTSB activity after 1 week of IGF-IIR/M6PR siRNA treatment. Cells were treated again using the two-hit combination 1 day prior to testing of CTSB activity. In the presence of IGF-IIR/M6PR siRNA, intracellular CTSB activity was depleted, indicating that IGF-IIR/M6PR is responsible for the increased endolysosomal targeting of CTSB.

tates (Fig. 9D). The KSHV-mediated increase in IGF-IIR/M6PR expression resulted in a concomitant increase in the level of coimmunoprecipitated CTSB.

To assess whether induced IGF-IIR/M6PR expression was responsible for the increased CTSB retention in the endosomal/lysosomal compartment in KSHV-infected cells, we treated KSHV-infected DMVEC with siRNA against IGF-IIR/M6PR. As shown in Fig. 9E, treatment with siRNA to IGF-IIR/M6PR efficiently reduced mRNA expression levels and had no effect on IGF-IR mRNA. Moreover, cell-associated CTSB activity was significantly reduced in cells treated with IGF-IIR/M6PR siRNA (Fig. 9F). Therefore, we conclude that IGF-IIR/M6PR is responsible for retaining active CTSB intracellularly by targeting CTSB to the endosomal/lysosomal compartment.

IGF-IIR/M6PR expression is required for DMVEC transformation by KSHV. To determine whether the IGF-IIR/M6PR-mediated retention of CTSB was essential for postconfluent growth and focus formation, we treated KSHV-infected DMVEC with IGF-IIR/M6PR siRNA. Cells were seeded at 30% confluence and incubated with three different siRNAs designed against IGF-IIR/M6PR. One week after the first treatment, cells were treated a second time with siRNA. At the end of 2 weeks, E-DMVEC treated with control siRNA (Cy3-labeled siRNA to luciferase) displayed the KSHV-mediated phenotypic change to a spindle cell phenotype. In contrast, all three individual IGF-IIR/M6PR-specific siRNAs efficiently inhibited spindle cell and focus formation (Fig. 10). Taken together with the finding that IGF-IIR/M6PR retained CTSB and that CTSB-specific siRNA inhibits KSHV-mediated postconfluent growth, these data strongly suggest that retention of CTSB by IGF-IIR/M6PR is essential for the development of the KSHV-induced tumorigenic phenotype.

DISCUSSION

CTSB involvement in tumorigenesis has been recognized in a variety of human tumors (48, 49, 51, 57), but this is the first

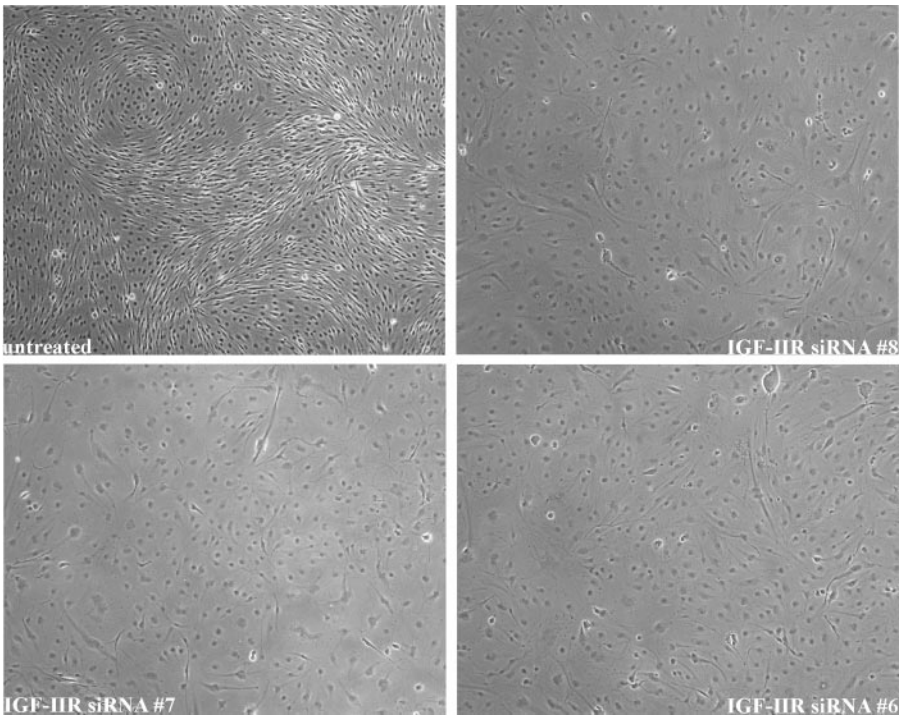

FIG. 10. IGF-IIR/M6PR siRNA inhibits spindle cell and focus formation in KSHV-infected E-DMVEC. Shown are representative phase-contrast microscopy images comparing untreated samples to IGF-IIR/M6PR siRNA-treated, KSHV-infected E-DMVEC. Control siRNA-treated samples were indistinguishable from untreated samples and are not represented here. IGF-IIR/M6PR siRNA reduced focus formation. Immunofluorescence analysis of Cy3-labeled siRNA transfectants indicated a transfection efficiency of >95% (data not shown).

time that CTSB has been implicated in KS. Latent infection by KSHV transforms immortalized DMVEC in a characteristic way that is reminiscent of observations of KS tumors: formation of LANA-positive spindle cells, loss of contact inhibition, continued proliferation postconfluence, formation of disorganized foci, and the ability to grow in soft agar. An essential function for CTSB in this transformation of E-DMVEC by KSHV was indicated by the finding that each of these steps was inhibited by the membrane-permeant methyl ester-modified CTSB inhibitor CA-074ME but not by the impermeant inhibitor CA-074. Both versions of CA-074 are specific for CTSB in vitro (Fig. 4B); however, the methyl ester modification reduces the specificity of CA-074ME for CTSB so that it also reacts with cathepsin L in tissue culture and in vivo (34). Treatment with siRNA specific for cathepsin L, B, or S revealed that only the inhibition of CTSB expression prevented KSHV-mediated postconfluent growth. These data strongly suggest that the inhibition of CTSB activity, but not that of cathepsin L activity, was responsible for the effect of CA-074ME. Interestingly, others have shown that treatment with the antisense strand of CTSB efficiently inhibited tumor invasion and angiogenesis in vitro and in mice (23, 25).

It has been documented in other tumor models that intracellular active CTSB can facilitate tumor invasion by acting intracellularly instead of being secreted (16, 49). For E-DMVEC latently infected with KSHV, we observed increased intracellular retention of CTSB concomitant with an increase in intracellular protease activity. CTSB splicing, transcript levels, and protein levels were unchanged by KSHV, with two dominant splice products being present, both missing exon 2 and one also missing exon 3 (Fig. 8B). The absence of exon 2 has previously been linked to a 15-fold increase in translational efficiency (1). CTSB lacking the sequence encoded by both exons does not enter the secretory pathway, since its signal sequence is also missing (32). Probing for active CTSB revealed that the majority of CTSB activity is located in vesicles, suggesting that CTSB is able to enter the vesicular sorting system and is likely sorted to the endosomal/lysosomal compartment. This is also supported by the finding that cell-associated CTSB activity is depleted upon disruption of lysosomal trafficking with NH_4Cl (Fig. 9). Therefore, E-DMVEC latently infected by KSHV display an increased diversion of CTSB from the exocytic route to the endolysosomal compartment.

Our data further suggest that increased endolysosomal targeting of CTSB resulted from increased retention by IGF-IIR/M6PR, which is transcriptionally induced in KSHV-infected cells. IGF-IIR/M6PR is not associated with any known downstream signaling cascade, because the receptor does not possess any signal transduction capacity. One of the functions of IGF-IIR/M6PR is to regulate IGF-II levels (36, 45). Increased release of IGF-II due to a loss of IGF-IIR/M6PR function has been implicated in the promotion of tumor growth in a variety of cancers (13, 14, 29, 40, 56). In addition, IGF-IIR/M6PR is known as the major cation-independent M6PR in endocytosis and intracellular trafficking of mannose 6-phosphate-tagged proteins, including endolysosomal proteases (13). The increased release of active proteases due to decreased expression of IGF-IIR/M6PR can contribute to tumor invasion of sur-

rounding tissues. This has been observed for human breast carcinoma, where increased secretion of cathepsin D correlated with a reduction in IGF-IIR/M6PR expression (3, 14, 29).

In contrast to the IGF-IIR/M6PR downregulation observed in many cancers, we previously noted an upregulation of IGF-IIR/M6PR in the context of a general KSHV-mediated dysregulation of the IGF system (43). We now demonstrate that this transcriptional increase of IGF-IIR leads to increased retention of CTSB. This conclusion is supported by coimmunoprecipitation and by the finding that siRNA treatment against IGF-IIR/M6PR depleted the concentration of active CTSB in KSHV-infected E-DMVEC (Fig. 9F). Furthermore, inhibition of IGF-IIR/M6PR expression by siRNA inhibited KSHV-mediated spindle cell and focus formation. Therefore, intracellular retention of CTSB by IGF-IIR is essential for KSHV-mediated postconfluent growth.

What is the potential role of intracellular CTSB in the development of KS spindle cells? Lysosomal CTSB is released into the cytosol in the presence of extrinsic stimuli of apoptosis, particularly tumor necrosis factor and tumor necrosis factor-related ligands, and cytosolic CTSB can act as an effector protease of programmed cell death in tumor cells (5, 12, 26). CTSB has also been identified as an inhibitor of p53-dependent apoptosis in a genome-wide screen of p53 modulators (17); however, death receptor-mediated apoptosis is inhibited by the KSHV protein vFLIP, which is expressed during latency (11). Moreover, if CTSB were promoting apoptosis, we would expect that inhibition of CTSB would prevent apoptosis. Inhibition of CTSB activity did not change the level of apoptosis in KSHV-infected cultures (Fig. 6B). Consequently, regulation of apoptosis is likely not to be involved in the observed function of CTSB in KS.

Another possible effect of CTSB inhibition could be interference with growth-promoting signal transduction cascades. This includes the regulation of IGF-dependent signaling, since cathepsins have been implicated in the cleavage of IGF-binding proteins (45). Indeed, we observed that cathepsins cleave the KSHV-induced IGFBP-2 (our unpublished observations). Therefore, it is conceivable that CTSB is involved in the previously described regulation of the IGF system by KSHV (43). Alternatively, CTSB could be involved in regulating other KSHV-induced protumorigenic host cell or viral factors. For instance, CTSB controls the processing and release of vascular endothelial growth factor (58), which plays an important role in KS (19).

Finally, CTSB could be involved in regulating the activity of matrix metalloproteases (MMP) (21) or other proteolytic processes. MMP and cysteine proteases play an important role in tumor invasion and angiogenesis by degrading various components of the extracellular matrix (24). CTSB has been shown to activate MMP (21). CTSB activity is generally a tightly controlled process, and deregulating CTSB during tumor growth may facilitate angiogenesis, invasion, or even loss of contact inhibition (18, 44, 47). Interestingly, MMP-1 and MMP-9 are induced in KSHV-infected E-DMVEC and have been shown to be essential for degrading various components of the extracellular matrix (A. V. Moses, unpublished observations). Moreover, an MMP inhibitor is in clinical trials for KS (7).

An imbalance in protease activity has been described for a wide range of diseases, including rheumatoid arthritis, osteoarthritis, cancer, neurological disorders, osteoporosis, and lysosomal storage diseases (21, 22, 53). Not surprisingly, 4 of the 11 characterized human cathepsins have been crystallized in an effort to aid structure-based drug design (52). Based on the data presented here, we suggest that CTSB would be a good target for treating KS.

ACKNOWLEDGMENTS

The work reported in this article was supported by grants 5R01-CA099906 and 5R01-CA94011-01 (to A.V.M. and K.F., respectively). M.B. was supported by grants R01-EB005011 and U54-RR020843. P.P.R. was supported by Molecular Hematology Training Grant T32 HL007781-13 and by an award from the American Heart Association.

Microarray assays (and/or data analysis) were performed in the Affymetrix Microarray Core/Spotted Microarray Core/Bioinformatics and Biostatistics Core of the OHSU Gene Microarray Shared Resource. We thank Aurelie Snyder of the OHSU-MMI Research Core Facility (http://www.ohsu.edu/research/core) for help with microscopy and Bala Chandran for his kind gift of the anti-LANA polyclonal antibody.

REFERENCES

1. **Baici, A., K. Muntener, A. Willimann, and R. Zwicky.** 2006. Regulation of human cathepsin B by alternative mRNA splicing: homeostasis, fatal errors and cell death. Biol. Chem. **387:**1017–1021.
2. **Berquin, I. M., L. Cao, D. Fong, and B. F. Sloane.** 1995. Identification of two new exons and multiple transcription start points in the 5′-untranslated region of the human cathepsin-B-encoding gene. Gene **159:**143–149.
3. **Berthe, M. L., M. Esslimani Sahla, P. Roger, M. Gleizes, G. J. Lemamy, J. P. Brouillet, and H. Rochefort.** 2003. Mannose-6-phosphate/insulin-like growth factor-II receptor expression levels during the progression from normal human mammary tissue to invasive breast carcinomas. Eur. J. Cancer **39:** 635–642.
4. **Boshoff, C., and Y. Chang.** 2001. Kaposi's sarcoma-associated herpesvirus: a new DNA tumor virus. Annu. Rev. Med. **52:**453–470.
5. **Bursch, W.** 2001. The autophagosomal-lysosomal compartment in programmed cell death. Cell Death Differ. **8:**569–581.
6. **Chapman, H. A., R. J. Riese, and G. P. Shi.** 1997. Emerging roles for cysteine proteases in human biology. Annu. Rev. Physiol. **59:**63–88.
7. **Cianfrocca, M., T. P. Cooley, J. Y. Lee, M. A. Rudek, D. T. Scadden, L. Ratner, J. M. Pluda, W. D. Figg, S. E. Krown, and B. J. Dezube.** 2002. Matrix metalloproteinase inhibitor COL-3 in the treatment of AIDS-related Kaposi's sarcoma: a phase I AIDS malignancy consortium study. J. Clin. Oncol. **20:**153–159.
8. **Dourmishev, L. A., A. L. Dourmishev, D. Palmeri, R. A. Schwartz, and D. M. Lukac.** 2003. Molecular genetics of Kaposi's sarcoma-associated herpesvirus (human herpesvirus-8) epidemiology and pathogenesis. Microbiol. Mol. Biol. Rev. **67:**175–212.
9. **Felbor, U., L. Dreier, R. A. Bryant, H. L. Ploegh, B. R. Olsen, and W. Mothes.** 2000. Secreted cathepsin L generates endostatin from collagen XVIII. EMBO J. **19:**1187–1194.
10. **Frlan, R., and S. Gobec.** 2006. Inhibitors of cathepsin B. Curr. Med. Chem. **13:**2309–2327.
11. **Guasparri, I., S. A. Keller, and E. Cesarman.** 2004. KSHV vFLIP is essential for the survival of infected lymphoma cells. J. Exp. Med. **199:**993–1003.
12. **Guicciardi, M. E., J. Deussing, H. Miyoshi, S. F. Bronk, P. A. Svingen, C. Peters, S. H. Kaufmann, and G. J. Gores.** 2000. Cathepsin B contributes to TNF-α-mediated hepatocyte apoptosis by promoting mitochondrial release of cytochrome *c*. J. Clin. Investig. **106:**1127–1137.
13. **Hawkes, C., and S. Kar.** 2004. The insulin-like growth factor-II/mannose-6-phosphate receptor: structure, distribution and function in the central nervous system. Brain Res. Brain Res. Rev. **44:**117–140.
14. **Hébert, E.** 2006. Mannose-6-phosphate/insulin-like growth factor II receptor expression and tumor development. Biosci. Rep. **26:**7–17.
15. **Hengge, U. R., T. Ruzicka, S. K. Tyring, M. Stuschke, M. Roggendorf, R. A. Schwartz, and S. Seeber.** 2002. Update on Kaposi's sarcoma and other HHV8 associated diseases. Part 1: epidemiology, environmental predispositions, clinical manifestations, and therapy. Lancet Infect. Dis. **2:**281–292.
16. **Hill, P. A., D. J. Buttle, S. J. Jones, A. Boyde, M. Murata, J. J. Reynolds, and M. C. Meikle.** 1994. Inhibition of bone resorption by selective inactivators of cysteine proteinases. J. Cell. Biochem. **56:**118–130.
17. **Huang, Q., A. Raya, P. DeJesus, S. H. Chao, K. C. Quon, J. S. Caldwell, S. K. Chanda, J. C. Izpisua-Belmonte, and P. G. Schultz.** 2004. Identification of p53 regulators by genome-wide functional analysis. Proc. Natl. Acad. Sci. USA **101:**3456–3461.
18. **Huet, G., R. M. Flipo, C. Colin, A. Janin, B. Hemon, M. Collyn-d'Hooghe, R. Lafyatis, B. Duquesnoy, and P. Degand.** 1993. Stimulation of the secretion of

latent cysteine proteinase activity by tumor necrosis factor alpha and interleukin-1. Arthritis Rheum. **36:**772–780.
19. **Im, E., A. Venkatakrishnan, and A. Kazlauskas.** 2005. Cathepsin B regulates the intrinsic angiogenic threshold of endothelial cells. Mol. Biol. Cell **16:** 3488–3500.
20. **Jenner, R. G., and C. Boshoff.** 2002. The molecular pathology of Kaposi's sarcoma-associated herpesvirus. Biochim. Biophys. Acta **1602:**1–22.
21. **Joyce, J. A., A. Baruch, K. Chehade, N. Meyer-Morse, E. Giraudo, F. Y. Tsai, D. C. Greenbaum, J. H. Hager, M. Bogyo, and D. Hanahan.** 2004. Cathepsin cysteine proteases are effectors of invasive growth and angiogenesis during multistage tumorigenesis. Cancer Cell **5:**443–453.
22. **Joyce, J. A., and D. Hanahan.** 2004. Multiple roles for cysteine cathepsins in cancer. Cell Cycle **3:**1516–1519.
23. **Krueger, S., C. Haeckel, F. Buehling, and A. Roessner.** 1999. Inhibitory effects of antisense cathepsin B cDNA transfection on invasion and motility in a human osteosarcoma cell line. Cancer Res. **59:**6010–6014.
24. **Lakka, S. S., C. S. Gondi, and J. S. Rao.** 2005. Proteases and glioma angiogenesis. Brain Pathol. **15:**327–341.
25. **Lakka, S. S., C. S. Gondi, N. Yanamandra, W. C. Olivero, D. H. Dinh, M. Gujrati, and J. S. Rao.** 2004. Inhibition of cathepsin B and MMP-9 gene expression in glioblastoma cell line via RNA interference reduces tumor cell invasion, tumor growth and angiogenesis. Oncogene **23:**4681–4689.
26. **Leist, M., and M. Jaattela.** 2001. Triggering of apoptosis by cathepsins. Cell Death Differ. **8:**324–326.
27. **Li, J. H., and J. S. Pober.** 2005. The cathepsin B death pathway contributes to TNF plus IFN-γ-mediated human endothelial injury. J. Immunol. **175:** 1858–1866.
28. **Livak, K. J., and T. D. Schmittgen.** 2001. Analysis of relative gene expression data using real-time quantitative PCR and the $2^{-\Delta\Delta C_T}$method. Methods **25:** 402–408.
29. **Lorenzo, K., P. Ton, J. L. Clark, S. Coulibaly, and L. Mach.** 2000. Invasive properties of murine squamous carcinoma cells: secretion of matrix-degrading cathepsins is attributable to a deficiency in the mannose 6-phosphate/insulin-like growth factor II receptor. Cancer Res. **60:**4070–4076.
30. **McAllister, S. C., S. G. Hansen, R. A. Ruhl, C. M. Raggo, V. R. DeFilippis, D. Greenspan, K. Fruh, and A. V. Moses.** 2004. Kaposi sarcoma-associated herpesvirus (KSHV) induces heme oxygenase-1 expression and activity in KSHV-infected endothelial cells. Blood **103:**3465–3473.
31. **McAllister, S. C., and A. V. Moses (ed.).** 2007. Endothelial cell- and lymphocyte-based in vitro systems for understanding KSHV biology. Springer Verlag, Heidelberg, Germany.
32. **Mehtani, S., Q. Gong, J. Panella, S. Subbiah, D. M. Peffley, and A. Frankfater.** 1998. In vivo expression of an alternatively spliced human tumor message that encodes a truncated form of cathepsin B. Subcellular distribution of the truncated enzyme in COS cells. J. Biol. Chem. **273:**13236–13244.
33. **Mohanam, S., S. L. Jasti, S. R. Kondraganti, N. Chandrasekar, S. S. Lakka, Y. Kin, G. N. Fuller, A. W. Yung, A. P. Kyritsis, D. H. Dinh, W. C. Olivero, M. Gujrati, F. Ali-Osman, and J. S. Rao.** 2001. Down-regulation of cathepsin B expression impairs the invasive and tumorigenic potential of human glioblastoma cells. Oncogene **20:**3665–3673.
34. **Montaser, M., G. Lalmanach, and L. Mach.** 2002. CA-074, but not its methyl ester CA-074Me, is a selective inhibitor of cathepsin B within living cells. Biol. Chem. **383:**1305–1308.
35. **Moore, P. S., and Y. Chang.** 2003. Kaposi's sarcoma-associated herpesvirus immunoevasion and tumorigenesis: two sides of the same coin? Annu. Rev. Microbiol. **57:**609–639.
36. **Moschos, S. J., and C. S. Mantzoros.** 2002. The role of the IGF system in cancer: from basic to clinical studies and clinical applications. Oncology **63:**317–332.
37. **Moses, A. V., K. N. Fish, R. Ruhl, P. P. Smith, J. G. Strussenberg, L. Zhu, B. Chandran, and J. A. Nelson.** 1999. Long-term infection and transformation of dermal microvascular endothelial cells by human herpesvirus 8. J. Virol. **73:**6892–6902.
38. **Moses, A. V., M. A. Jarvis, C. Raggo, Y. C. Bell, R. Ruhl, B. G. Luukkonen, D. J. Griffith, C. L. Wait, B. J. Druker, M. C. Heinrich, J. A. Nelson, and K. Fruh.** 2002. A functional genomics approach to Kaposi's sarcoma. Ann. N. Y. Acad. Sci. **975:**180–191.
39. **Moses, A. V., M. A. Jarvis, C. Raggo, Y. C. Bell, R. Ruhl, B. G. Luukkonen, D. J. Griffith, C. L. Wait, B. J. Druker, M. C. Heinrich, J. A. Nelson, and K. Fruh.** 2002. Kaposi's sarcoma-associated herpesvirus-induced upregulation of the c-*kit* proto-oncogene, as identified by gene expression profiling, is essential for the transformation of endothelial cells. J. Virol. **76:**8383–8399.
40. **O'Gorman, D. B., J. Weiss, A. Hettiaratchi, S. M. Firth, and C. D. Scott.** 2002. Insulin-like growth factor-II/mannose 6-phosphate receptor overexpression reduces growth of choriocarcinoma cells in vitro and in vivo. Endocrinology **143:**4287–4294.
41. **Palmer, J. T., D. Rasnick, J. L. Klaus, and D. Bromme.** 1995. Vinyl sulfones as mechanism-based cysteine protease inhibitors. J. Med. Chem. **38:**3193–3196.
42. **Raggo, C., R. Ruhl, S. McAllister, H. Koon, B. J. Dezube, K. Fruh, and A. V. Moses.** 2005. Novel cellular genes essential for transformation of endothelial cells by Kaposi's sarcoma-associated herpesvirus. Cancer Res. **65:**5084–5095.
43. **Rose, P. P., J. M. Carroll, P. A. Carroll, V. R. Defilippis, M. Lagunoff, A. V. Moses, C. T. Roberts, Jr., and K. Früh.** 2007. The insulin receptor is essential for virus-induced tumorigenesis of Kaposi's sarcoma. Oncogene **26:**1995–2005.
44. **Roshy, S., B. F. Sloane, and K. Moin.** 2003. Pericellular cathepsin B and malignant progression. Cancer Metastasis Rev. **22:**271–286.
45. **Scharf, J. G., and T. Braulke.** 2003. The role of the IGF axis in hepatocarcinogenesis. Horm. Metab. Res. **35:**685–693.
46. **Schwartz, R. A., and W. C. Lambert.** May 2006, posting date. Kaposi sarcoma. Emedicine from WebMD. http://www.emedicine.com/derm/topic203.htm.
47. **Sloane, B., K. Moin, M. Sameni, L. Tait, J. Rozhin, and G. Ziegler.** 1994. Membrane association of cathepsin B can be induced by transfection of human breast epithelial cells with c-Ha-ras oncogene. J. Cell Sci. **107:**373–384.
48. **Sloane, B. F., S. Yan, I. Podgorski, B. E. Linebaugh, M. L. Cher, J. Mai, D. Cavallo-Medved, M. Sameni, J. Dosescu, and K. Moin.** 2005. Cathepsin B and tumor proteolysis: contribution of the tumor microenvironment. Semin. Cancer Biol. **15:**149–157.
49. **Szpaderska, A. M., and A. Frankfater.** 2001. An intracellular form of cathepsin B contributes to invasiveness in cancer. Cancer Res. **61:**3493–3500.
50. **Thurmond, R. L., S. Sun, L. Karlsson, and J. P. Edwards.** 2005. Cathepsin S inhibitors as novel immunomodulators. Curr. Opin. Investig. Drugs **6:**473–482.
51. **Turk, B., D. Turk, and V. Turk.** 2000. Lysosomal cysteine proteases: more than scavengers. Biochim. Biophys. Acta **1477:**98–111.
52. **Turk, D., and G. Guncar.** 2003. Lysosomal cysteine proteases (cathepsins): promising drug targets. Acta Crystallogr. D **59:**203–213.
53. **Turk, V., J. Kos, and B. Turk.** 2004. Cysteine cathepsins (proteases)—on the main stage of cancer? Cancer Cell **5:**409–410.
54. **Turk, V., B. Turk, and D. Turk.** 2001. Lysosomal cysteine proteases: facts and opportunities. EMBO J. **20:**4629–4633.
55. **Wang, H. W., M. W. Trotter, D. Lagos, D. Bourboulia, S. Henderson, T. Makinen, S. Elliman, A. M. Flanagan, K. Alitalo, and C. Boshoff.** 2004. Kaposi sarcoma herpesvirus-induced cellular reprogramming contributes to the lymphatic endothelial gene expression in Kaposi sarcoma. Nat. Genet. **36:**687–693.
56. **Wang, Z. Q., M. R. Fung, D. P. Barlow, and E. F. Wagner.** 1994. Regulation of embryonic growth and lysosomal targeting by the imprinted Igf2/Mpr gene. Nature **372:**464–467.
57. **Yan, S., and B. F. Sloane.** 2003. Molecular regulation of human cathepsin B: implication in pathologies. Biol. Chem. **384:**845–854.
58. **Yanamandra, N., K. V. Gumidyala, K. G. Waldron, M. Gujrati, W. C. Olivero, D. H. Dinh, J. S. Rao, and S. Mohanam.** 2004. Blockade of cathepsin B expression in human glioblastoma cells is associated with suppression of angiogenesis. Oncogene **23:**2224–2230.